RADIOPHYSICS

Original article
DOI: https://doi.org/10.18721/JPM.15314

SYNTHESIS OF WINDOW FUNCTIONS FOR REDUCING SYSTEMATIC ERRORS OF MULTIPLEXED FIBER-OPTIC SENSORS

A. A. Markvart✉, *L. B. Liokumovich, N. A. Ushakov*

Peter the Great St. Petersburg Polytechnic University, St. Petersburg, Russia

✉ markvart_aa@spbstu.ru

Abstract. In the paper, the systematic (bias) error of digital processing of the biharmonic signal of two multiplexed fiber-optic interferometers under spectral interrogation, when the registered spectral transfer function being processed through a discrete Fourier transform has been analyzed. The synthesis of a special weighted window function was put forward; this made it possible to reduce the systematic errors in determining the frequencies of a polyharmonic signal without a significant increase in the random (noise) error. The effectiveness of this approach was proven through numerical simulation and experimentally by comparison with the error when using standard Dolph − Chebyshev window. The proposed approach can be applied in any problems related to the estimation of frequencies and phases of polyharmonic signals.

Keywords: harmonic analysis, discrete Fourier transform, methodological error, window function, interferometer

Funding: The reported study was carried out as a part of the State Assignment for Fundamental Research (Subject Code FSEG-2020-0024).

Citation: Markvart A. A., Liokumovich L. B., Ushakov N. A., Synthesis of window functions for reducing systematic errors of multiplexed fiber-optic sensors, St. Petersburg State Polytechnical University Journal. Physics and Mathematics. 15 (3) (2022) 185–200. DOI: https://doi.org/10.18721/JPM.15314

Научная статья
УДК 535.3, 535-15, 535.417
DOI: https://doi.org/10.18721/JPM.15314

СИНТЕЗ ОКОННЫХ ФУНКЦИЙ ДЛЯ СНИЖЕНИЯ МЕТОДИЧЕСКИХ ОШИБОК МУЛЬТИПЛЕКСИРОВАННЫХ ВОЛОКОННО-ОПТИЧЕСКИХ ДАТЧИКОВ

А. А. Маркварт✉, *Л. Б. Лиокумович*, *Н. А. Ушаков*

Санкт-Петербургский политехнический университет Петра Великого,

Санкт-Петербург, Россия

✉ markvart_aa@spbstu.ru

Аннотация. Проведен анализ методической погрешности цифровой обработки бигармонического сигнала двух мультиплексированных волоконно-оптических интерферометров при спектральном опросе, когда регистрируемая спектральная передаточная функция обрабатывается посредством дискретного преобразования Фурье. Предложен синтез специальной весовой оконной функции, позволяющей снизить методические погрешности определения частот полигармонического сигнала без существенного увеличения случайной погрешности. Эффективность такого подхода доказана численным моделированием и экспериментально, путем сравнения с результатами применения стандартного окна Дольфа – Чебыш□ва. Предложенный подход может использоваться в любых задачах, связанных с оценкой частот и фаз полигармонических сигналов.

Ключевые слова: гармонический анализ, дискретное преобразование Фурье, методическая погрешность, оконная функция, интерферометр.

Финансирование: Работа выполнена в рамках Государственного задания на проведение фундаментальных исследований (код темы FSEG-2020-0024).

Ссылка для цитирования: Маркварт А. А., Лиокумович Л. Б., Ушаков Н. А. Синтез оконных функций для снижения методических ошибок мультиплексированных волоконно-оптических датчиков // Научно-технические ведомости СПбГПУ. Физико-математические науки. 2022. Т. 15. № 3. С. 185–200. DOI: https://doi.org/10.18721/JPM.15314

Introduction

Fiber-optic sensors are the focus of much attention in R&D, due to their high accuracy, immunity to electromagnetic interference, compact size, and capabilities for multiplexing and remote interrogation [1]. Such sensors can measure various physical impacts, such as temperature, stretching, pressure, etc., and have a wide range of applications, from monitoring buildings and structures to medical diagnostics.

One type of such sensors are interferometric fiber optic sensors [2]. Spectral interferometry is an effective widespread mechanism for interrogating these sensors. It involves recording and subsequently processing the dependence of the relative intensity level of the light S passed through a sensitive interferometer on the frequency f of this light; this dependence $S(f)$ is the spectral transfer function (SPF) of this interferometer [3].

Users generally tend to multiplex two or more interferometers connected to a single interrogation setup [4, 5]. Importantly, the STF of multiplexed interferometers contains sums of harmonic components with certain frequencies and phases characterizing each of the sensing elements; this can be confirmed experimentally.

The most common approach to processing STF applies the discrete Fourier transform (DFT) with analysis of the resulting harmonic components. However, the spectral leakage effect produces systematic errors in determining the frequencies and phases of harmonic components in STF and, consequently, errors in demodulation of signals from multiplexed sensors and their parasitic interference. Standard weight functions, e.g., Hamming, Kaiser, Blackman, Dolph–Chebyshev windows, are commonly used to reduce the level of these errors. [6, 7]. Their drawback is a decrease in spectral resolution and an increase in the influence of noise on measurements due to increased equivalent noise bandwidth (ENBW) of the window. Therefore, it is worth considering synthesis of specialized windows reducing demodulation errors without a significant deterioration in ENBW level. This approach was considered in [8–10] and used in radar systems. However, the algorithm proposed by the authors for synthesizing the window and finding the harmonic component frequencies of the signal is multi-iterative, which means that the windows have to be recalculated with any change in these frequencies. The frequencies of the harmonic components in STF only vary slightly in measurements using fiber optic interferometers. This allows avoiding iterative recalculation of windows, using a single weight window specifically synthesized for a particular scheme.

This paper proposes a method for reducing demodulation errors in signals from two multiplexed fiber-optic interferometric sensors by synthesizing a specialized weight window.

The proposed method has none of these drawbacks which are inherent in the existing methods for synthesizing windows.

Circuit description and general principles for synthesizing the special window

For certainty, we consider a circuit with two multiplexed sensing elements, which are the so-called extrinsic fiber Fabry–Perot interferometers (EFFPI), Fig. 1) [3, 8]. Each EFFPI is formed by the endface of a single-mode waveguide feed and a mirror with an air gap between them, with thicknesses L_1 and L_2 for the first and second EFFPI, respectively. The variations L_1 and L_2 from the measured quantity (deformation, temperature, etc.) are to be determined in the measurements. The radiation of the frequency (or wavelength) tunable laser passes through the circulator and is directed through the coupler to both EFFPIs, is s reflected from them, entering the photodetector through the coupler and the circulator.

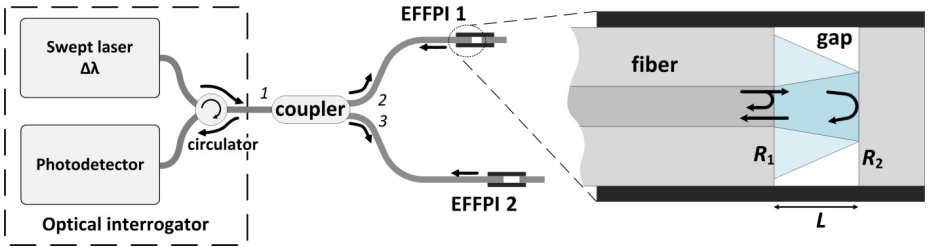

Fig. 1. Measuring circuit with multiplexed EFFPI:
Optical interrogator; swept laser; circulator; coupler with ports *1*, *2* and 3; fiber; interferometer gap with the width L; photodetector; R_1, R_2 are the reflectivities of the mirrors

We consider the case of low-finesse EFFPIs (valid for small R_1 and R_2), when multiply reflected waves can be omitted. If the difference in the lengths of the feeding fiber segments between the EFFPI and the coupler is greater than the coherence length of the radiation source, the STF is determined by the interference of beam pairs from each EFFPI [4, 11]:

$$S\left(f, L_1, L_2\right) = \overline{S} + S_1 \cos\left[\frac{4\pi L_1}{c} f + \gamma_1\left(L_1\right)\right] + S_2 \cos\left[\frac{4\pi L_2}{c} f + \gamma_2\left(L_2\right)\right], \quad (1)$$

where

$$\overline{S} = \alpha_{12}^2\left[R_1 + R_2\eta_1\right] + \alpha_{13}^2\left[R_1 + R_2\eta_2\right],$$

$$S_{1,2} = 2\alpha_{12,13}^2 \sqrt{R_1 R_2 \eta_{1,2}},$$

$$\eta_{1,2} = \frac{\pi^2 w_0 \left(f\right)^2}{L_{1,2}^2 c^2 / f^2 + \pi^2 w_0 \left(f\right)^2},$$

$$\gamma_{1,2} = \pi - \text{arctg}\left(\frac{L_{1,2}}{z_R}\right),$$

$$z_R = \pi \cdot f \cdot w_0^2 \left(f\right) / c.$$

The following notations are adopted in Eq. (1): f, c are the frequency and speed of light; S is the mean STF level; $S_{1,2}$ are the amplitudes of interference components determined by mirrors $R_{1,2}$, coupling coefficients $\alpha_{12,13}$ of the coupler and light losses in the EFFPI due to divergence of light in the gap (losses are taken into account by the coefficients $\eta_{1,2}$); $\gamma_{1,2}$ are the phase shifts of waves; z_R is the Rayleigh length of the Gaussian beam; w_0 is the waist radius of the Gaussian beam.

The waves acquire a phase shift upon reflection from the external mirror, as well as due to divergence of light in the interferometer gap. The explicit form of expressions for $\eta_{1,2}$ and $\gamma_{1,2}$ is obtained via a Gaussian beam model for light in the interferometer gap [11] (z_R is Rayleigh length of the Gaussian beam); the waist radius of the Gaussian beam corresponds to the radius of the fiber mode spot. Notably, STF calculations in small frequency-tuning ranges used in practical interrogation devices generally neglect minor variations in the values of $\eta_{1,2}$, $\gamma_{1,2}$, z_R and w_0 due to variation in frequency f.

In practice, the interrogation system records a set of readouts $S_i = S(f_i, L_1, L_2)$, where i is the readout number. A uniform frequency step Δ is taken for further processing. If f_0 is the center of the frequency scanning range and N is the number of readouts, then

$$f_i = f_0 + [i - (N-1)/2] \cdot \Delta, \tag{2}$$

where i varies from 0 to $(N-1)$ and the scanning range $\Delta f = \Delta \cdot (N-1)$.

Demodulation of the obtained dependence $S(f)$ consists in finding the values of L_1 and L_2, which in turn amounts to estimating the frequencies and phases of the harmonic components of the following sequence:

$$v\left(i\right) = w\left(i\right)\left\{\overline{S} + S_1 \cos\left[\omega_1\left(L_1\right) \cdot i + \vartheta_1\left(L_1\right)\right] + S_2 \cos\left[\omega_2\left(L_2\right) \cdot i + \vartheta_2\left(L_2\right)\right]\right\}, \tag{3}$$

where $w(i)$ is the weighting window used; $\omega_{1,2}(L_{1,2})$ are the circular frequencies in radians; $\vartheta_{1,2}(L_{1,2})$ are the phases of harmonic components.

In view of expressions (1) and (2), we obtain:

$$\omega_{1,2}(L_{1,2}) = 4\pi\Delta \cdot L_{1,2}/c, \tag{4}$$

$$\vartheta_{1,2}\left(L_{1,2}\right) = 4\pi \cdot f_0 \cdot L_{1,2} / c - 2\pi \cdot \Delta \cdot \left(N-1\right) \cdot L_{1,2} / c + \gamma_{1,2}\left(L_{1,2}\right). \tag{5}$$

The Fourier transform of the sequence of counts (3) takes the form [6]:

$$\begin{aligned} V\left(\omega, L_1, L_2\right) &= \overline{S} \cdot W\left(\omega\right) + \\ &+0.5 \cdot S_1 \cdot \exp\left[j\vartheta_1\left(L_1\right)\right] \cdot W\left[\omega - \omega_1\left(L_1\right)\right] + 0.5 \cdot S_1 \cdot \exp\left[-j\vartheta_1\left(L_1\right)\right] \cdot W\left[\omega + \omega_1\left(L_1\right)\right] + \\ &+0.5 \cdot S_2 \cdot \exp\left[j\vartheta_2\left(L_2\right)\right] \cdot W\left[\omega - \omega_2\left(L_2\right)\right] + 0.5 \cdot S_2 \cdot \exp\left[-j\vartheta_2\left(L_2\right)\right] \cdot W\left[\omega + \omega_2\left(L_2\right)\right], \end{aligned} \tag{6}$$

where $W(\omega)$ is the Fourier transform of the window $w(i)$.

The frequencies $\omega_{1,2}$ are typically found by determining the positions $\omega_{1m,2m}$ of the peaks on the Fourier transform modulus V, and the phases $\vartheta_{1,2}$ are found by calculating the argument V in these peaks (taking into account the influence of the window). However, it can be seen from expression (3) that the first, third, fourth and fifth terms generate errors for the values of ω_1 and θ_1. This is because the second term with $W(0)$ required for estimating the magnitude of the quantity $|V(\omega)|$ and the argument V in the region ω_1 is supplemented by the terms with $W(\omega_1)$, $W(2\omega_1)$, $W(\omega_1 - \omega_2)$ and with $W(\omega_1 + \omega_2)$, distorting the result. Similarly, the first, second, third and fifth terms generate errors for the values of ω_2 and θ_2 found in region ω_2. To determine the frequencies and phases correctly, we should synthesize such a weight window w^{synt} whose Fourier transform W^{synt} could minimize the corresponding parasitic components in the required frequency frequency range, due to dips in W^{synt} in the regions ω_1, $2\omega_1$, $(\omega_1 + \omega_2)$, $(\omega_1 - \omega_2)$, ω_2, $2\omega_2$, $(\omega_2 - \omega_1)$. Furthermore, additional dips in W^{synt} should also be provide in the negative frequency range, so that the Fourier transform W^{synt} is symmetrical relative to zero, because the frequency estimate by the maxima of the Fourier transform $|V|$ of the sequence multiplied by the window w^{synt} is unbiased only in this case. The additional frequencies for the negative range are $-\omega_1$, $-2\omega_1$, $-(\omega_1 + \omega_2)$, $-\omega_2$, $-2\omega_2$.

Thus, the quantity W^{synt} should be minimized in the range of the above 12 frequencies, i.e., in the bands $\Delta\Omega_p$, $p = \pm1, \pm2, ..., \pm6$, accounting for the potential variation in the frequencies $\omega_{1,2}$ with respect to the variation in $L_{1,2}$, as well as the shift in the positions $\omega_{1m,2m}$ of the maxima $|V|$ due to spectral leakage and the influence of the noise from the measuring equipment. Denoting these variations in frequency as $\Delta\omega_1$ and $\Delta\omega_2$, we can write the following expressions for the zeros in W^{synt}:

$$\Delta\Omega_{\pm1} = \Delta\omega_1,\ \Delta\Omega_2 = {}_{\pm}\Delta\omega_1,\ \Delta\Omega_{\pm3} = \Delta\omega_2,$$

$$\Delta\Omega_{\pm4} = 2\Delta\omega_2,\ \Delta\Omega_{\pm5} = \Delta\omega_1 + \Delta\omega_2,\ \Delta\Omega_{\pm6} = \Delta\omega_1 + \Delta\omega_2.$$

It is preferable to synthesize the required window $w^{synt}(i)$ based on one of the standard windows $w(i)$,, introducing an additional requirement for a minimum residual of the Fourier transforms $W^{synt}(\omega)$ and $W(\omega)$ of these windows outside these regions. In this case, the requirements for the window $w^{synt}(i)$ can be written as two conditions:

$$\begin{cases} \text{Condition 1:} \\ \left|W^{synt}(\omega)\right| \to \min \text{ for} \\ \quad \omega \in \pm\left[\omega_{1m} - \Delta\Omega_1/2;\ \omega_{1m} + \Delta\Omega_1/2\right] \cup \pm\left[2\omega_{1m} - \Delta\Omega_2/2;\ 2\omega_{1m} + \Delta\Omega_2/2\right] \cup \\ \qquad \cup \pm\left[\omega_{2m} - \Delta\Omega_3/2;\ \omega_{2m} + \Delta\Omega_3/2\right] \cup \pm\left[2\omega_{2m} - \Delta\Omega_4/2;\ 2\omega_{2m} + -\Delta\Omega_4/2\right] \cup \\ \qquad \cup \pm\left[\omega_{1m} - \omega_{2m} - \Delta\Omega_5/2;\ \omega_{1m} - \omega_{2m} + \Delta\Omega_5/2\right] \cup \\ \qquad \cup \pm\left[\omega_{1m} + \omega_{2m} - \Delta\Omega_6/2;\ \omega_{1m} + \omega_{2m} + \Delta\Omega_6/2\right]; \\ \text{Condition 2:} \\ \left|W^{\text{synt}}(\omega) - W(\omega)\right| \to \min \text{ for other } \omega. \end{cases} \tag{7}$$

Condition 1 gives the dips of W^{synt} at frequencies $\pm\omega_1$, $\pm2\omega_1$, $\pm\omega_2$, $\pm2\omega_2$, $\pm|(\omega_1 - \omega_2)|$, $\pm(\omega_1 + \omega_2)$. Notice that it is this condition (7) that is responsible for suppressing $W^{synt}(\omega)$ in the given frequency ranges and is in fact aimed at reducing the systematic error in finding the frequencies and phases of the harmonic components due to the parasitic effects described above.

The second condition can be interpreted as minimization of the broadening in the main Fourier transform lobe of the window. It prevents an increase in the ENBW value of the window, i.e., an increase in the random measurement error due to noise from the measuring equipment.

There are different approaches to tgenerating dips in the Fourier transform of a certain sequence of readouts. Such approaches are the best developed for antenna arrays, often involving synthesis of the discrete amplitude-phase distribution of currents over the elements of the antenna array to produce dips in the antenna's directivity pattern in the given directions [12–15]. We use the approach to solving this problem outlined in [15], as it is relatively simple. According to this

approach, the required Fourier transform of the window W^{synt} is represented as the difference of the initial W and compensating W^{comp} Fourier transforms:

$$W^{synt} = W - W^{comp}. \tag{8}$$

The window is synthesized by the following logic. For example, let the compensating transform W^{comp} be the window transform whose main lobe is frequency-shifted to the position ω_1 and is equal in amplitude to the magnitude of the initial transform W at this point. Then, a zero of the transform W^{synt} appears after subtraction at the point ω_1. Broad dips can be produced by generating a set of zeros at multiple points ω_k filling the regions with dips. The compensating Fourier image is composed as a sum [15]:

$$W^{\text{comp}}(\omega) = \sum_{k=1}^{K} H_k \cdot G(\omega - \omega_k), \tag{9}$$

where $G(\omega)$ are the basic functions; $\{\omega_k\}$ is a set of frequency points generating zeros in the Fourier transform of the synthesized window; $\{H_k\}$ are the coefficients before basis functions, calculated after the set $\{\omega_k\}$ is given.

The Fourier transform of a rectangular window is used as the basis function. The synthesized function W^{synt} is obtained by finding the set $\{\omega_k\}$. The coefficients $\{H_k\}$ are calculated from the condition that the value of the subtracted function W^{comp} be equal to the value of the initial function W at each of the points of the set $\{\omega_k\}$. This condition can be written in the following matrix form:

$$\left[W(\omega_k)\right] = \left[W^{\text{comp}}(\omega_k)\right] \cdot \left[H_k\right]. \tag{10}$$

Then the coefficients $\{H_k\}$ can be found using the expression

$$\left[H_k\right] = \left[W^{\text{comp}}(\omega_k)\right]^{-1} \cdot \left[W(\omega_k)\right]. \tag{11}$$

After these coefficients are calculated, the search window $w^{synt}(i)$ is found by an inverse Fourier transform with respect to W^{synt}, or, in view of the theorem on the frequency shift of a Fourier transform, using the expression

$$w^{\text{comp}}(i) = \sum_{k=1}^{K} H_k \cdot g(i) \cdot \exp\left[j\omega_k i\right]. \tag{12}$$

where $g(i)$ is the inverse Fourier transform of the basis function $G(\omega)$.

Method for finding the optimal set $\{\omega_k\}$

The crucial step within the proposed approach is to select the set $\{\omega_k\}$ to best satisfy condition (7). A simple version was used in [15, 16], with an equidistant distribution of a certain number of points ω_k in the regions assumed to have dips in the Fourier transform W^{synt}. However, this choice may be far from optimal. Multiparameter optimization is actually required, where the parameters optimized include not only the values of ω_k but also the number of points K in the set. To solve the problem, we consider some target function M. It is logical to introduce minimization of the highest levels of $|W^{synt}|$ in the regions with dips into this function, as well as the regularization term r, depending on the magnitude of ENBW:

$$\begin{cases} M = \max\left|W^{\text{synt}}\left[\omega_{1\text{m}} - \Delta\Omega_1/2\,;\omega_{1\text{m}} + \Delta\Omega_1/2\right]\right| + \max\left|W^{\text{synt}}\left[2\omega_{1\text{m}} - \Delta\Omega_2/2;\, 2\omega_{1\text{m}} + \Delta\Omega_2/2\right]\right| + \\ + \max\left|W^{\text{synt}}\left[\omega_{2\text{m}} - \Delta\Omega_3/2;\, \omega_{2\text{m}} + \Delta\Omega_3/2\right]\right| + \max\left|W^{\text{synt}}\left[2\omega_{2\text{m}} - \Delta\Omega_4/2;\, 2\omega_{2\text{m}} + \Delta\Omega_4/2\right]\right| + \\ + \max\left|W^{\text{synt}}\left[\left|\omega_{1\text{m}} - \omega_{2m}\right| - \Delta\Omega_5/2;\, \left|\omega_{1\text{m}} - \omega_{2m}\right| + \Delta\Omega_5/2\right]\right| + \\ + \max\left|W^{\text{synt}}\left[\omega_{1\text{m}} + \omega_{2m} - \Delta\Omega_6/2;\, \omega_{1\text{m}} + \omega_{2m} + \Delta\Omega_6/2\right]\right| + \\ + r\left\{\text{ENBW}\left(w^{\text{synt}}\right)\right\}. \end{cases} \tag{13}$$

As mentioned above, an increase in the depth of the dips is accompanied by the increase in ENBW, therefore, we should aim to compromise between these values, that is, between the systematic and random errors; the required balance can be regulated by selecting the function $r\{\mathrm{ENBW}(w^{synt})\}$. It is preferable to select the actual points ω_k in regions that are slightly wider (by k times) than $\Delta\Omega_p$, i.e., with the width of $k{\cdot}\Delta\Omega_p$.

In this paper, we used a genetic optimization algorithm [17] to find the set $\{\omega_k\}$, since it is well suited for a problem where the target function defined by expression (13) is considerably nonlinear with multiple discontinuities. The optimization procedure was carried out in the MATLAB software package using the built-in ga function with a random set $\{\omega_k\}$ in the first generation [18]. In view of the symmetry requirements for W^{Synt}, the set $\{\omega_k\}$ was taken to be symmetric with respect to zero. The enerations had a length of $K/2$ because the values of ω_k were optimized in the region of positive frequencies due to symmetry. The minimization function was programmed so that not only the position ω_k but also the value of K was optimized. On the one hand, the higher K, the deeper the dips W^{Synt} formed; on the other hand, however, the condition number of the matrix $[\underline{W}^{comp}(\omega_k)]$ is reduced, producing computational errors and incorrect results. The initial value of K and the population size were selected empirically. The remaining parameters of the ga function were selected by default.

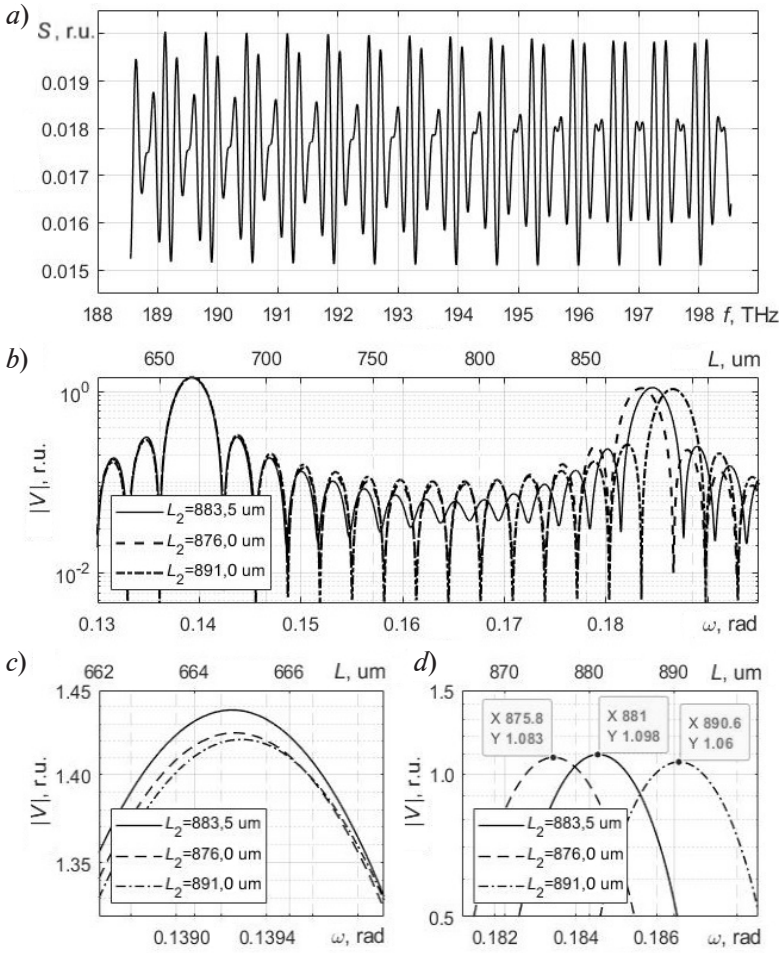

Fig. 2. Numerical simulation of biharmonic signal from two multiplexed fiber-optic interferometers: *a* shows the STF frequency dependence for the circuit; *b* shows the dependences $|V(\omega)|$; *c*, *d* show fragments of $|V(\omega)|$; L_1 = 664.8 μm, L_2 = 883.5 μm (*a*); L_1 = 664.8 μm, the values of L_2 are given in the captions (*b*–*d*)

Demonstration of the proposed approach based on simulation

To illustrate the results of the proposed approach and reduce the systematic error of signal demodulation from multiplexed EFFPIs, we carried out numerical simulation in the MATLAB software package. The spectral transfer function $S(f)$ was calculate by Eq. (1) in the frequency range $\Delta f = 9.99$ THz with the center of the frequency scanning range $f_0 = 193.54$ THz (this corresponds to the range from 1510 to 1590 nm in the wavelength scale), the frequency step $\Delta = 5$ GHz and readout number $N = 2000$. The mirror reflectivities $R_{1,2} = 3.5\%$ were used as the parameters of the multiplexed EFFPIs. The value $w_0 = 5.2$ μm (corresponding to the mode field diameter (MFD) of a standard single-mode fiber for a wavelength of 1550 nm), assumed to be fixed, was selected for the Gaussian beam radius used in expression (1). Based on these values, we calculated a set of readout sequences $S(f)$ (5001 sequences); the gap L_1 of the first EFFPI was taken to be constant, with $L_1 = 664.8$ μm, and the gap L_2 of the second EFFPI was linearly increased from one STF to another in the range from 861 to 906 μm at a step of 10 nm. Notice that the given simulation parameters were selected based on the experimental data (described and analyzed below). Fig. 2, *a* shows a graph of the calculated STF for $L_2 = 883.5$ μm.

The mean STF was found from the calculated readouts, with the sequence then centered for subsequent signal processing. This was done to minimize the parasitic effect from the constant component of STF on the results of signal processing by DFT. Next, a 200,000-point DFT $V(\omega)$ was calculated for each centered STF. A rectangular single window $w(i) = 1$ was chosen as the initial one, where $i = 1, 0, N - 1$. Its Fourier transform is found by the following formula:

$$W(\omega) = \frac{\sin(\omega N/2)}{\sin(N/2)} \exp\left[-j\omega(N-1)/2\right]. \quad (14)$$

Fig. 2,*b* shows variation in $|V(\omega)|$ for three values of L_2: 876.0, 883.5 and 891.0 μm at $L_1 = 664.8$ μm. In addition to the frequency scale in radians, a scale L values in μm was added to the figure for convenience (recalculated using expression (4)). Evidently, the position of the maxima $|V(\omega)|$ deviates from the given values of L_1 and L_2, pointing to the systematic error in determining the gap lengths.

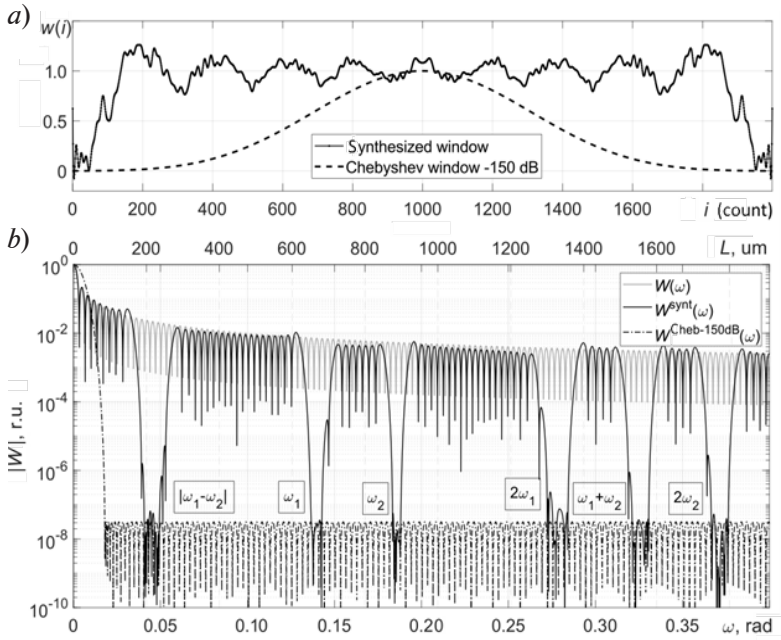

Fig. 3. Comparison of dependences for the window we synthesized and the standard Dolph–Chebyshev window: *a* shows the dependences of w on the readout number; *b* shows the normalized dependences of the Fourier transform magnitude. for $w(i)$, $w^{synt}(i)$ and $w^{\text{Cheb-150dB}}(i)$

Next, following the above algorithm, we synthesized the window w^{synt} satisfying condition (7). The Fourier transform function of a rectangular window was selected as the basis for calculating the window by Eqs. (8), (9), i.e., $G(\omega) = W(\omega)$. To find the optimal set $\{\omega_k\}$, the function $r\{\mathrm{ENBW}(w^C)\}$ in condition (13) was take to equal zero, since in this case the value of the ENBW window during synthesis was close to unity.

The window w^{synt} was synthesized assuming that the sensor gap varied within the range of 15 μm with the centers $L_{10} = 664.8$ μm, $L_{20} = 883.5$ μm. The following parameters in condition (13) were selected for these parameters of the optical circuit:

circular frequencies $\omega_1 = 0.1392$ rad and $\omega_2 = 0.1851$ rad;
frequency bands $\Delta\omega_1 = \Delta\omega_2 = 0.0034$ rad.

These values of the bands correspond to the above gap variation range plus a margin of 1 μm, taken to account for the potential displacement due to systematic error (the displacement was estimated from the data in Fig. 2, *b*–*d*). The following parameters were adopted for genetic optimization:

population size 500; number of points in the set $\{\omega_k\}$ $K/2 = 90$;
coefficient $k = 2$.

Fig. 3 shows graphs of the synthesized window (weight function) $w^{synt}(i)$ and the Fourier-transformed $W^{synt}(\omega)$ obtained with this window. Apparently, six deep dips were obtained at the level of at least $3\cdot10^{-8}$ relative to the maximum of the main lobe. Outside the dip region, the dependence $W^{synt}(\omega)$ is close to the Fourier transform of the rectangular window $W(\omega)$ shown in this figure. The main lobe broadened insignificantly in this case. The ENBW value for w^{synt} was 1.0737, compared to a unit ENBW (1.000) for a rectangular window.

Notably, the same nulls in the side lobes can be obtained using standard windows. For example, it is convenient to compare the synthesized window with the Dolph–Chebyshev window, since the latter allows setting an arbitrary level for the side lobes, which are located at the same level in the entire frequency band. To obtain dips at a level of about $3\cdot10^{-8}$, we should use the Dolph–Chebyshev window with a side lobe level of -150dB (we denote it as $w^{\text{Cheb-150dB}}$, and its Fourier transform as $W^{\text{Cheb-150dB}}$), whose ENBW value is 1.9814, which is 1.8 times higher than that of the synthesized window $w^{synt}(\omega)$. Moreover, the optimization algorithm apparently reduced the level of $K/2$ to 58 from the initial value of 90, indicating that it was chosen correctly.

The set of functions $S(f)$ was used to calculate the corresponding dependences $V(\omega)$. Then, the positions of L_{1m} and L_{2m} of two main maxima were found for each $V(\omega)$, taking into account expression (4). They were found by interpolating the parabola at the three maximum points $|V(\omega)|$ in the region of the peak and determining its vertex. Similarly, the positions of the two main maxima L_{1m}^{synt} and L_{2m}^{synt} were found for all $V(\omega)$. The maxima were recalculated from the set of STF and multiplied by the window w^{synt}. In addition, the positions of peaks in $L_{1m}^{\text{Cheb-150dB}}$ and $L_{2m}^{\text{Cheb-150dB}}$ were found for $|V(\omega)|$ by multiplying STF by the window $w^{\text{Cheb-150dB}}$. The results are shown in Fig. 4.

It is clear from the graphs in Fig. 4, *a* and *c* that the systematic error in determining L_1 and L_2 with a rectangular window has a pronounced oscillating character. The period of rapid oscillations is associated with the variation in L, resulting in a phase shift of the harmonic by 2π in the sequence $v(i)$. The period of slow oscillations is due to displacement of the parasitic side lobe system relative to the frequency of the target maximum $V(w)$.

Importantly, the oscillations were successfully reduced by five orders of magnitude for the selected gap variation range using the synthesized window: this can be seen from comparing the graphs in Fig. 4, *a* and *b*, as well as Fig. 4, *c* and *d*.

The window $w^{\text{Cheb-150dB}}$ yields the same reduction (see Fig. 4, *b* and *d*), eliminating the drawback of the standard window that consists in increased ENBW value, since no noise was introduced in this simulation.

Experimental demonstration of the proposed approach

The proposed approach was tested through an experiment using the scheme discussed above (see Fig. 1). Each EFFPI was constructed using two patch cords with SMF-28 fiber, spliced with APC-type (tapered) connectors on one side and UPC-type (straight) connectors on the other.

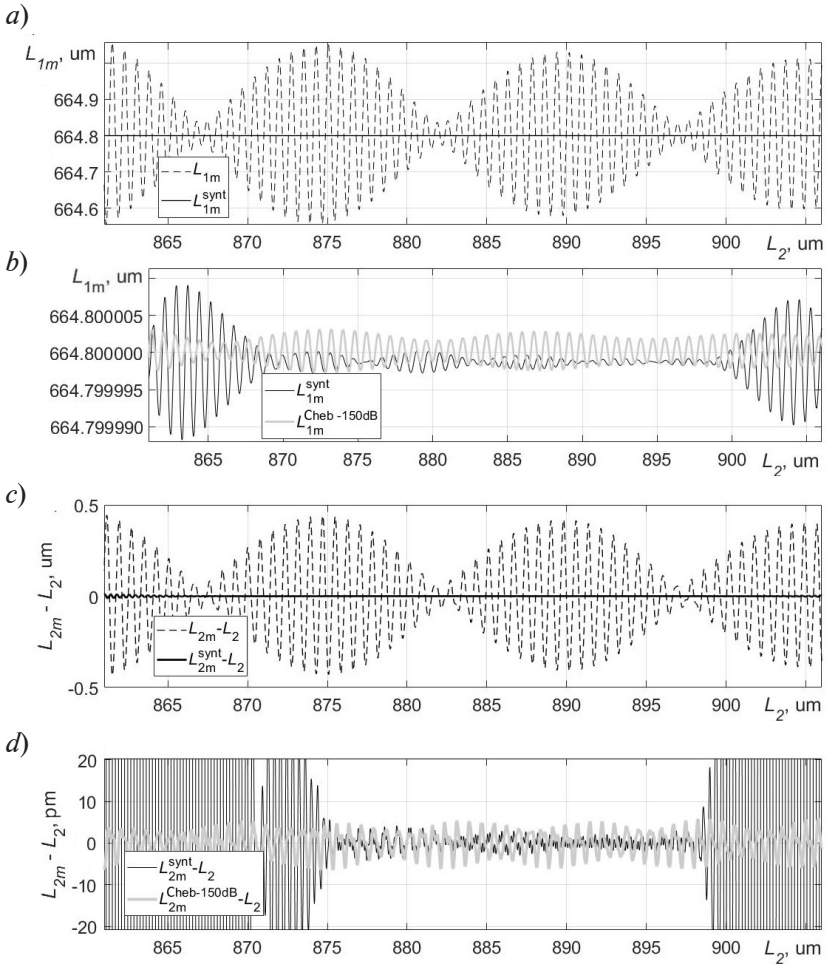

Fig. 4. Positions of the main maxima as function of given L_2 value: L_{1m} and L_{1m}^{synt} (*a*), L_{1m}^{synt} and $L_{1m}^{\text{Cheb-150dB}}$ (*b*), $L_{2m} - L_2$ and $L_{2m}^{synt} - L_2$ (*c*), $L_{2m}^{synt} - L_2$ and $L_{1m}^{\text{Cheb-150dB}} - L_2$ (*d*)

The straight ends of the patchcords were combined with a gap in a standard connector plug. Thus, the reflection coefficients at the quartz/air boundary were $R \approx \%3.5$. One of the patchcords was connected to a 50:50 coupler, and the other was left free; the parasitic reflections of light from this end of the patchcord were negligible (due to the tapered end). The first port of the coupler was connected to the optical interrogator NI-PXIe-4844, which was capable of detecting STF in the range of 1510–1590 nm with a uniform wavelength step of 4 pm. The appearance of the experimental setup is shown in Fig. 5,*a*.

The gap of the first EFFPI was set to approximately $L_1 = 664.8$ μm during the experiment, and subsequently left unchanged. The gap of the second EFFPI was slowly reduced from 906 to 861 μm. The recorded STFs were then interpolated from a uniform wavelength scale to a uniform optical frequency scale with the range $\Delta f = 9.99$ THz, the band center $f_0 = 193.54$ THz, the frequency step $\Delta = 5$ GHz and the number of readouts $N = 2000$. Fig. 5, *b* shows an example of the obtained $S(f)$ for the values $L_1 \approx 664.8$ μm and $L_2 \approx 906$ μm. The mean value was found from the obtained STF readouts; the sequence was then centered and its Fourier transform $V(\omega)$ determined by DTF. Fig. 5,*c* shows an example of the resulting function $|V(\omega)|$ for the same values of L_1 and L_2.

The positions L_{1m} and L_{2m} of the two main maxima $|V(\omega)|$ were found for each dependence $V(\omega)$. The function $V(\omega)$ was also determined for the STF multiplied by the synthesized window w^{synt} (the same as in the simulation), and the positions of the two main maxima L_{1m}^{synt} and L_{2m}^{synt} were found. The computational results are shown in Fig. 6,*a* and *b*.

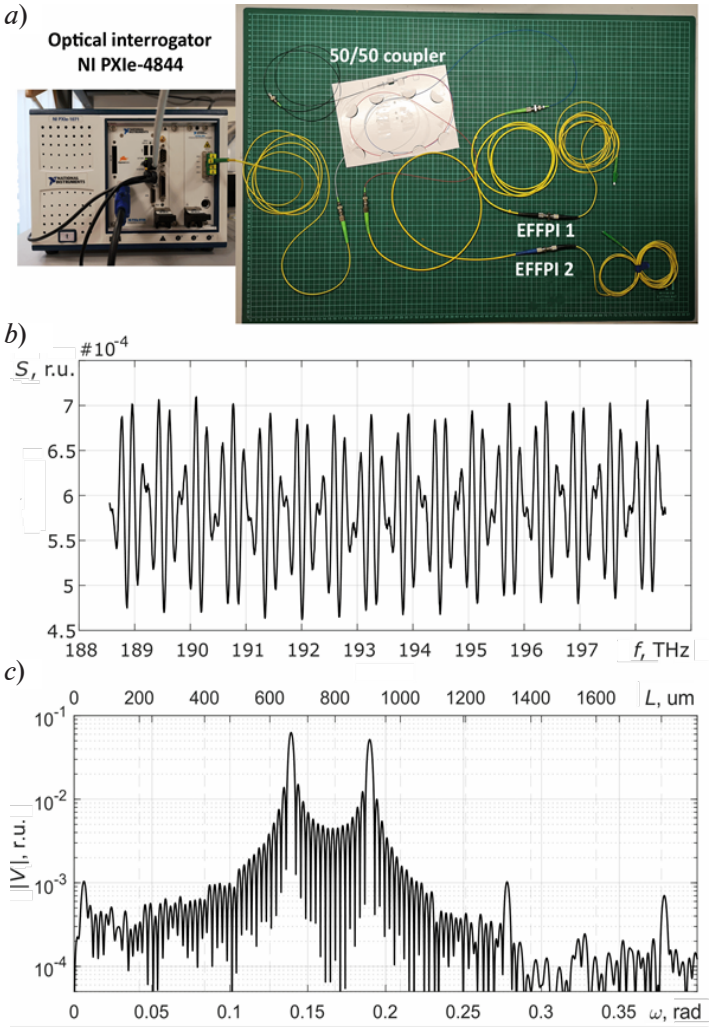

Fig. 5. Photograph of experimental setup (*a*) and examples of experimental data obtained: dependencies $S(f)$ (*b*) and $|V(\omega)|$ (*c*) for $L_1 \approx 664.8$ μm and $L_2 \approx 906$ μm

Table

Error estimation: comparison of results in the presence of noise-generated error

Window (weight function)	σ_{L1m}, nm	ENBW value
Rectangular	8.3. (noise only) 121	1.0000
Synthesized	9.0	1.0737
Dolph–Chebyshev: –60 dB	17.0	1.5180
–70 dB	13.4	1.6336
–80 dB	14.0	1.7432
–90 dB	15.0	1.8445
–100 dB	16.1	1.9414

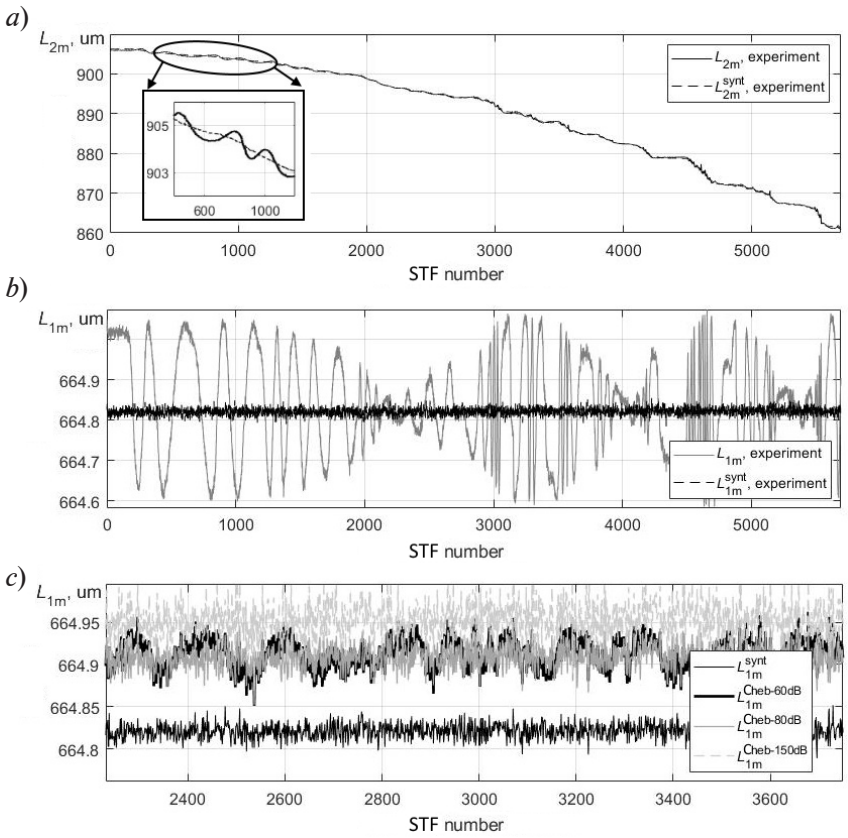

Fig. 6. Processed experimental dependences on the STF number: positions of the main peaks L_{2m} and L_{2m}^{synt} (*a*), L_{1m} and L_{1m}^{synt} (*b*), L_{1m}^{synt}, $L_{1m}^{\text{Cheb-60dB}}$, $L_{1m}^{\text{Cheb-80dB}}$, $L_{1m}^{\text{Cheb-150dB}}$ (*c*)

As seen from Fig. 6, *a*, the value of L_{2m} decreases from one STF to another; the reason for non-uniform variation in L_{2m} is that the gap L_2 was decreased manually. As predicted by the simulation results, this decrease is accompanied by an oscillating error of finding the value of L_{1m}, as can be clearly seen in Fig. 6, *b*. A synthesized window allowed to virtually suppress the oscillating error, which follows from the nature of the L_{1m}^{synt} curve in the same figure. Moreover, suppression of the oscillating error is also clear from comparing the L_{2m} and L_{2m}^{synt} curves (see the inset in Fig. 6,*a*).

Unlike the simulation results, noise is observed in the experiment, which demonstrates the advantage of the synthesized window over the standard ones.

Let us analyze the results obtained for suppressing the systematic error in the presence of the noise-induced error. As noted earlier, the advantage of the synthesized window is a slight increase in the ENBW value compared to standard windows. The analysis was carried out for the values found for L_{1m}. The RMS error of L_{1m} upon variation in L_2 (i.e., in the presence of oscillations due to systematic error) with a rectangular window was $\sigma_{L1m} = 121$ nm. The RMS error of L_{1m}^{synt} with the synthesized window was $\sigma_{L1msynt} = 9$ nm. Thus, the RMS error of the values of L_{1m} found with varying L_2 decreased by 13 times, starting to depend mainly on the noise from the measuring equipment.

Only the noise error can be estimated for the region where the value of L_2 remained unchanged (the first 100 STFs recorded). In this case, the values obtained are $\sigma_{L1m\_noise} = 8.2$ nm and $\sigma_{L1msynt} = 8.7$ nm, i.e., the noise increment is insignificant (by only 1.06 times). Recall that the ENBW value of the synthesized window is 1.07 times higher than that of the rectangular one. These results are summarized in Table.

In addition to the presented analysis, let us compare the effectiveness of the approach using a synthesized window with the standard one considering the example of the Dolph–Chebyshev window. To this end, we additionally defined the values of L_{1m}^{Cheb}using Dolph–Chebyshev windows

with different levels of side lobes (three dependences of this type are shown in Fig. 6,*c*). As seen from the figure, the systematic error prevails over the noise error at the level of -60 dB, becoming less noticeable against the increased noise error at the level of -80 dB; it is not detected at all at the level of -150 dB. The results for this analysis of the quantity L_{1m}^{Cheb} are also given in Table. The obtained data indicate that the minimum value of RMS error (σ_{L1m}) among the L_{1m}^{Cheb} found is observed for the level of -70 dB and is equal to $\sigma_{L1m\text{Cheb}} = 13.4$ nm. This level reflects the trade-off between systematic bias and noise figure. In this particular case, a synthesized window yielded RMS deviations that were 1.49 times better than for the measurements carried out with a standard Dolph–Chebyshev window at -70 dB. Notably, the ENBW value of the synthesized window was lower by 1.52 times.

Fig. 6 shows that the values of L found experimentally have different constant offsets with different windows, which was not observed in numerical simulations and, generally speaking, is a factor of the constant error in demodulation. One possible reason for the difference is that the noise present in the recorded STFs is not white; the other option is that additional parasitic harmonics (for example, from parasitic interferometers in the fiber-optic channel) may be present in the signal and exert some influence. However, search for the causes of this effect is a subject for separate study and is beyond the scope of our paper.

Conclusion

We have analyzed the problems of signal demodulation in interferometric fiber-optic systems with multiplexed interferometric sensors during spectral interrogation with the recorded STF processed by DTF. Both simulation and experiments confirmed the presence of a considerable systematic error in measuring the frequencies of harmonic components of STF. A specially synthesized weight window is proposed as a solution for reducing the systematic error without a significant increase in the noise error. A specific example was considered numerically and experimentally to confirm the effectiveness of the proposed approach compared to the standard Dolph–Chebyshev window. The procedure proposed can be used in any problems related to estimation of frequencies and phases of polyharmonic signals.

REFERENCES

1. **Udd E., Spillman. Jr. W. B.** (Eds.), Fiber optic sensors: An introduction for engineers and scientists, 2nd ed., John Wiley & Sons Inc., New York, 2011.

2. **Liokumovich L. B.**, Volokonno-opticheskiye interferometricheskiye izmereniya [Fiber optic interferometric measurements], Polytech. University Press, St. Petersburg, 2007 (in Russian).

3. **Ushakov N., Liokumovich L.** Resolution limits of extrinsic Fabry – Perot interferometric displacement sensors utilizing wavelength scanning interrogation // Appl. Optics. 53 (23) (2014) 5092-5099.

4. **Ushakov N. A., Liokumovich L. B.,** Multiplexed extrinsic fiber Fabry –Pérot interferometric sensors: resolution limits, J. Lightwave Technol. 33 (9) (2015) 1683–1690.

5. **Ushakov N. A., Markvart A. A., Liokumovich L. B.,** Pulse wave velocity measurement with multiplexed fiber optic Fabry – Pérot interferometric sensors, IEEE Sens. J. 20 (19) (2020) 11302–11312.

6. **Oppenheim A. V., Schafer R. W.,** Discrete-time signal processing, 2nd ed., Pearson Education, London, 2007.

7. **Dvorkovich V. P., Dvorkovich A. V.,** Okonnyye funktsii dlya garmonicheskogo analiza signalov [Window functions for harmonic signal analysis, 2nd ed.], Tekhnosfera Publishing, Moscow, 2016 (in Russian).

8. **Baranov I. V., Ezerski V. V.,** Minimization to inaccuracy of the measurement of the distance under digital processing signal in FM radar for industrial application], Bulletin of Ryazan State Radioengineering University. (24) (2008) 55–60.

9. **Davydochkin V. M.,** Vesovyye funktsii i algoritmy dlya povysheniya tochnosti otsenki chastoty i amplitudy vyborki garmonicheskogo signala na fone signalopodobnykh pomekh, Avtoref. dis. kand. tekhn. nauk [Weighting functions and algorithms for improving the accuracy of estimating the frequency and amplitude of a harmonic signal sample against the background of signal-like noise], Synopsis of Thesis for Cand. Techn. Sci., Ryazan, 2008.

10. **Davydochkin V. M., Davydochkina S. V.,** Window functions for the digitial adaptive harmonic analysis of the signals with the miltimodal spectrum, J. Radioengineering. (9) (2009) 11–20 (in Russian).

11. **Markvart A. A., Liokumovich L. B., Ushakov N. A.,** Estimating the measurement resolution of an arbitrary finesse fiber-optic Fabry – Perot interferometer via Cramer – Rao bound, St. Petersburg Polytechnical State University Journal. Physics and Mathematics. 14 (4) (2021) 172–189.

12. **Zelkin E. G., Sokolov V. G.,** Metody sinteza antenn: Fazirovannyye antennyye reshetki i antenny s nepreryvnym raskryvom [Antenna synthesis methods: Phased antenna array and antennas with continuous aperture], Sovetskoye Radio Publishing, Moscow, 1980 (in Russian).

13. **Mangoud M. A.-A., Elragal H. M.,** Antenna array pattern synthesis and wide null control using enhanced particle swarm optimization, Progr. Electromagn. Res. B. 17 (2009) 1–14.

14. **Vendik O. G., Kalinin S. A., Kozlov D. S.**, Phased array with controlled directivity pattern, Techn. Phys. 58 (10) (2013) 1507–1511.

15. **Kozlov D. S.,** Interferentsionnoye formirovaniye diagrammy napravlennosti fazirovannoy antennoy reshetki s podavleniyem izlucheniya v zadannom napravlenii s uchetom vzaimnogo vliyaniya izluchateley. Avtoref. dis. kand. fiz.-mat. nauk [Interference beamforming of a phased antenna array with suppression of radiation in a given direction, taking into account the mutual influence of emitters], Synopsis of Thesis for Cand. Phys.-Math. Sci., St. Petersburg, 2016.

16. **Markvart A. A., Ushakov N. A., Liokumovich L. B.**, Application of weight window synthesis in a discrete Fourier transform to reduce demodulation errors of signals of multiplexed fiber-optic sensors, In book: Proc. 24-th Int. Conf. "Digital Signal Processing and its Applications" (DSPA-2022), Publ. by A. S. Popov Russian Scientific and Technical Society of Radio Engineering, Electronics and Communications Press. (24) (2022) 177–182.

17. **Sivanandam S. N., Deepa S. N.,** Introduction to genetic algorithms, Berlin, Heidelberg, Springer, 2008.

18. MathWorks Help Center. Genetic Algorithm, https://www.mathworks.com/help/gads/genetic-algorithm.html, Accessed June 01, 2022.

СПИСОК ЛИТЕРАТУРЫ

1. Волоконно-оптические датчики. Вводный курс для инженеров и научных работников. Под ред. Э. Удда. Пер. с англ. М.: Техносфера, 2008. 520 с.

2. Лиокумович **Л. Б.** Волоконно-оптические интерферометрические измерения. СПб.: Изд-во Политехнического ун-та, 2007. 110 с.

3. **Ushakov N., Liokumovich L**. Resolution limits of extrinsic Fabry – Perot interferometric displacement sensors utilizing wavelength scanning interrogation // Applied Optics. 2014. Vol. 53. No. 23. Pp. 5092–5099.

4. **Ushakov N. A., Liokumovich L. B.** Multiplexed extrinsic fiber Fabry – Perot interferometric sensors: resolution limits // Journal of Lightwave Technology. 2015. Vol. 33. No. 9. Pp. 1683–1690.

5. **Ushakov N. A., Markvart A. A., Liokumovich L. B.** Pulse wave velocity measurement with multiplexed fiber optic Fabry – Pérot interferometric sensors // IEEE Sensors Journal. 2020. Vol. 20. No. 19. Pp. 11302–11312.

6. **Оппенгейм А., Шафер Р.** Цифровая обработка сигналов. 3-е изд. Пер. с англ. М.: Техносфера, 2007. 1048 с.

7. **Дворкович В. П., Дворкович А. В.** Оконные функции для гармонического анализа сигналов. 2-е изд. М.: Техносфера, 2016. 217 с.

8. **Баранов И. В., Езерский В. В.** Минимизация погрешности измерения расстояния при цифровой обработке сигналов частотных дальномеров промышленного применения // Вестник Рязанского государственного радиотехнического университета. 2008. № 24. С. 55–60.

9. **Давыдочкин В. М.** Весовые функции и алгоритмы для повышения точности оценки частоты и амплитуды выборки гармонического сигнала на фоне сигналоподобных помех. Автореф. дис. канд. техн. наук. Рязань: Академия права и управления ФСИН, 2008. 16 с.

10. **Давыдочкин В. М., Давыдочкина С. В.** Весовые функции для цифрового адаптивного гармонического анализа сигналов с многомодовым спектром // Радиотехника. 2009. № 9. С. 11–20.

11. **Маркварт А. А., Лиокумович Л. Б., Ушаков Н. А.** Соотношение Рао – Крамера для оценки разрешающей способности измерений с волоконно-оптическим интерферометром Фабри – Перо произвольной добротности // Научно-технические ведомости СПбГПУ. Физико-математические науки. 2021. Т. 14. № 4. С. 172–189.

12. **Зелкин Е. Г., Соколов В. Г.** Методы синтеза антенн: фазированные антенные решетки и антенны с непрерывным раскрывом. М.: Советское радио, 1980. 294 с.

13. **Mangoud M. A.-A., Elragal H. M.** Antenna array pattern synthesis and wide null control using enhanced particle swarm optimization // Progress in Electromagnetics Research B. 2009. Vol. 17. Pp. 1–14.

14. **Вендик О. Г., Калинин С. А., Козлов Д. С.** Фазированная антенная решетка с управляемой формой диаграммы направленности // Журнал технической физики. 2013. Т. 83. № 10. С. 117–121.

15. **Козлов Д. С.** Интерференционное формирование диаграммы направленности фазированной антенной решетки с подавлением излучения в заданном направлении с учетом взаимного влияния излучателей. Автореф. дис. канд. физ.-мат. наук. СПб: ЛЭТИ, 2016. 16 с.

16. Маркварт **А. А., Ушаков Н. А.,** Лиокумович **Л. Б.** Применение синтеза весовых окон в дискретном преобразовании Фурье для снижения ошибок демодуляции сигналов мультиплексированных волоконно-оптических датчиков // Сборник трудов 24-й Международной конференции «Цифровая обработка сигналов и ее применение» (DSPA-2022). Вып. 24. М.: Изд-во РНТОРЭС имени А. С. Попова, 2022. С. 177–182.

17. **Sivanandam S. N., Deepa S. N.** Introduction to genetic algorithms. Berlin, Heidelberg: Springer, 2008. 442 p.

18. MathWorks Help Center. Genetic Algorithm. Режим доступа: https://www.mathworks.com/help/gads/genetic-algorithm.html (Дата обращения: 01.06.2022).

THE AUTHORS

MARKVART Aleksandr A.
Peter the Great St. Petersburg Polytechnic University
29 Politechnicheskaya St., St. Petersburg, 195251, Russia
markvart_aa@spbstu.ru
ORCID: 0000-0001-8080-0830

LIOKUMOVICH Leonid B.
Peter the Great St. Petersburg Polytechnic University
29 Politechnicheskaya St., St. Petersburg, 195251, Russia
leonid@spbstu.ru
ORCID: 0000-0001-5988-1429

USHAKOV Nikolai A.
Peter the Great St. Petersburg Polytechnic University
29 Politechnicheskaya St., St. Petersburg, 195251, Russia
n.ushakoff@spbstu.ru
ORCID: 0000-0002-3480-2779

СВЕДЕНИЯ ОБ АВТОРАХ

МАРКВАРТ Александр Александрович – *ассистент Высшей школы прикладной физики и космических технологий Санкт-Петербургского политехнического университета Петра Великого.*
195251, Россия, г. Санкт-Петербург, Политехническая ул., 29
markvart_aa@spbstu.ru
ORCID: 0000-0001-8080-0830

ЛИОКУМОВИЧ Леонид Борисович – *доктор физико-математических наук, профессор Высшей школы прикладной физики и космических технологий Санкт-Петербургского политехнического университета Петра Великого.*
195251, Россия, г. Санкт-Петербург, Политехническая ул., 29
leonid@spbstu.ru
ORCID: 0000-0001-5988-1429

УШАКОВ Николай Александрович – *кандидат физико-математических наук, доцент Высшей школы прикладной физики и космических технологий Санкт-Петербургского политехнического университета Петра Великого.*
195251, Россия, г. Санкт-Петербург, Политехническая ул., 29
n.ushakoff@spbstu.ru
ORCID: 0000-0002-3480-2779

Received 20.06.2022. Approved after reviewing 16.08.2022. Accepted 16.08.2022.
Статья поступила в редакцию 20.06.2022. Одобрена после рецензирования 16.08.2022. Принята 16.08.2022.